Equivalent exploitation of four-pulse one-dimensional ESEEM and HYSCORE spectroscopies for the elucidation of BOHC defects in borate glasses supported by quantum mechanical calculations

George Kordas*

Sol-Gel Laboratory of Glass and Ceramics, Institute of Materials Science, National Center for Scientific Research "Demokritos," 15310 Aghia Paraskevi Attikis, Greece

(Received 6 September 2002; revised manuscript received 15 April 2003; published 14 July 2003)

B_2O_3-Li_2O glass was exposed to ^{60}Co γ irradiation and measured with four-pulse (4P) one-dimensional (1D) electron spin echo envelop modulation (ESEEM) spectroscopy and hyperfine sublevel correlation (HYSCORE) spectroscopy. 4P 1D ESEEM revealed the values of $\chi_{zz} \leqslant 0.7$ MHz, $\eta \sim 0.4$ $T_{\text{aniso}} \leqslant 0.8$ MHz, and $A_{\text{iso}} \sim 0.6$ MHz for the second boron neighbor. In a- and c-B_2O_3, 4P 1D ESEEM uncovered the value of $\chi_{zz} \sim 2.6$ MHz for the second boron neighbor. HYSCORE spectroscopy in the B_2O_3-Li_2O glass revealed a weak coupling with $\chi_{zz} \leqslant 0.7$ MHz, $\eta \sim 0.37$, $T_{\text{aniso}} \leqslant 0.9$ MHz, and $A_{\text{iso}} \leqslant 0.9$ MHz due to the interaction of the spin with the second boron neighbor loosely bonded with the defect. An orthoborate group in the proximity of fourfold coordinated boron cluster reproduces the experimental parameters most satisfactorily.

DOI: 10.1103/PhysRevB.68.024202 PACS number(s): 61.43.Fs, 61.80.Ed, 61.72.Hh

I. INTRODUCTION

Electron paramagnetic resonance (EPR) spectroscopy has been used for the characterization of the paramagnetic states occurring in the alkali borate and borosilicate glasses.[1-19] This research was motivated by both technological (fiber optics, nuclear waste materials, etc.)[15-17] and scientific (e.g., boron anomaly)[18] incentives. As of today, two centers are known to exist in the borate glasses, the one named as center I and the other center II. Lately, they have been renamed as $BOHC_1$ (center I) and $BOHC_2$ (center II) occurring at alkali metal concentration the one below 25 mol % and the other above 25 mol %, respectively.[1,16] Table I presents the spectroscopic parameters of these defects.

In the last few years, advanced EPR techniques have been employed for the characterization of the $BOHC_1$.[7-16] This center was described by a hole trapped by nonbridging oxygen bonded to a threefold coordinated boron.[7] This triangle is part of the boroxol ring or attached to two boroxol rings or one boroxol ring.[7-14] These three variants can be distinguished by the name $BOHC_{1\alpha}$, $BOHC_{1\beta}$, and $BOHC_{1\gamma}$, respectively. This concept was confirmed by 1D ESEEM spectroscopy,[15,16] recently.

On the other hand, there is no sustainable model for the structure of the $BOHC_2$. At present, two models have been proposed for the $BOHC_2$.[16] In the first model, a hole is trapped on the $-BO_2^{2-}$ ● group.[6,19] In the second model, a hole is trapped by nonbridging oxygen bonded to threefold coordinated boron connected over the bridging oxygens to two fourfold coordinated boron ions.[16]

This work make use of 4P 1D ESEEM (Refs. 20–23) and HYSCORE (Refs. 7–14, 24–26) spectroscopies in the a- and c-B_2O_3 and 1 B_2O_3 1 Li_2O glass in order to acquire additional data useful for the development of a structural model for the $BOHC_2$. A number of structures were calculated using the G98W program to estimate the resultant A, T, and Q tensors[27] and to select one suitable structure. The visualization of the results was performed with the GAUSS VIEW WINDOWS package. The B3LYP method and the EPR-III basis set were used for these calculations.[27,28] The EPR-III basis set was optimized for boron.[29]

II. EXPERIMENTAL

Borate glasses were prepared by melting H_3BO_3 and Li_2CO_3 in a platinum crucible at temperatures between 800–1200 °C. The glasses were exposed to ^{60}Co irradiation (1500 Curie source) for ten hours to induce paramagnetic states. The FT-EPR spectra were recorded by a 300 E Bruker ESP 380 X-Band instrument equipped with a Bruker ESP380-1078 IN echo integrator. The instrument dead time was about 100 nsec. The temperature was set at <25 K using

TABLE I. Spectroscopic parameters of the $BOHC_1$ and $BOHC_2$ occurring in borate glasses (Ref. 1).

Defect	g_1	g_2	g_3	A_1 (G/MHz)	A_2 (G/MHz)	A_3 (G/MHz)	A_{iso} (G/MHz)
Center I (<25 mol %)	2.0020	2.0103	2.0350	12.1	14.2	10.0	12.1
($BOHC_1$)				33.9	40.0	28.5	34.1
Center II (>25 mol %)	2.0049	2.0092	2.0250	11.2	12.9	8.0	10.7
($BOHC_2$)				31.4	36.3	22.7	30.1

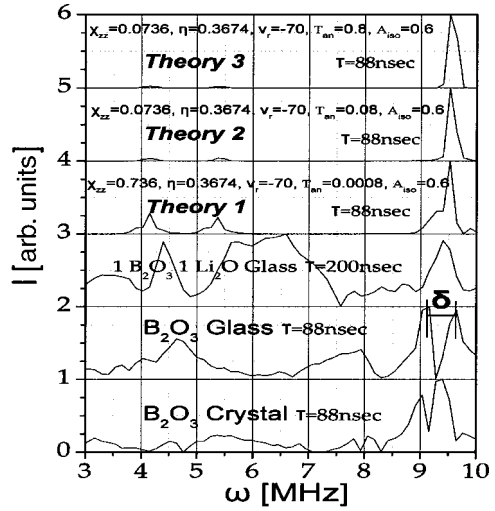

FIG. 1. 4P 1D ESEEM recorded in the B_2O_3, B_2O_3 Li_2O glasses and B_2O_3 crystal compared with three theoretical curves using the parameters of Table II. The simulation was accomplished using a program developed in house, the concept of which has been described in a previous paper. Parameters for the simulation of the 4P 1D ESEEM spectrum $g_x=2.0049$, $g_y=2.0092$, $g_z=2.0250$, $B=3420$ G, $A_{\rm iso}=0.6$ MHz, $\eta=0.37$, and $\angle v\ (g\text{-}Q)=70°$. Theory 1: χ_{zz} [MHz]$=0.74$ and $T_{\rm aniso}$ [MHz]$=0.0008$. Theory 2: χ_{zz} [MHz]$=0.074$ and $T_{\rm aniso}$ [MHz]$=0.08$.

an Oxford Instrument cryostat. The microwave frequency was measured using a HP 5350B counter. The HYSCORE spectra were recorded using the sequence

$$\frac{\pi}{2}(16\ \text{nsec})-\tau(104,168,240\ \text{nsec})-\frac{\pi}{2}(16\ \text{nsec})$$
$$-t_1[56+dt(=16\text{nsec})]-\pi\ (32\ \text{nsec})$$
$$-t_2[56+dt(=16\ \text{nsec})]-\frac{\pi}{2}(16\ \text{nsec})-\text{echo}.$$

The 4P 1D ESEEM spectra were recorded with $\tau=88$ nsec incremented by $d\tau=16$ nsec for another time sweep dt. Phase cycling was employed to remove the unwanted echoes in the Bruker Pulse Spel library.

III. RESULTS

A. 4P 1D ESEEM

Figure 1 shows the 4P 1D ESEEM spectrum of the B_2O_3 Li_2O glass, B_2O_3 glass, and B_2O_3 crystal. The structures of a- and c-B_2O_3 were investigated by FT-EPR and pulse ENDOR spectroscopies.[7–14] The NQC parameter for a- and c-B_2O_3 is equal to $\sim$2.7 MHz for the second neighbor.[7] Boron occurs with two isotopes, namely, the ^{11}B(80.2 n.a., $\omega_I=4.67$ MHz, $2^*\omega_I=9.34$ MHz, $H=3.42$ G) and the ^{10}B(19.8 n.a., 1.565 MHz, $2^*\omega_I=3.13$ MHz, $H=3.42$ G). These two isotopes are expected to generate 4P 1D ESEEM peaks (Fig. 1) at $\nu_\alpha(^{11}\text{B},\ ^{10}\text{B})$, $\nu_\beta(^{11}\text{B},\ ^{10}\text{B})$, and $\nu_\alpha(^{11}\text{B},\ ^{10}\text{B})\pm\nu_\beta(^{11}\text{B},\ ^{10}\text{B})$ frequencies.[22,23] Additionally, the ^{7}Li(92.5 n.a., $\omega_I=5.66$ MHz, $2^*\omega_I=11.32$ MHz) peaks should also be present in the $B_2O_3Li_2O$ glass. Indeed, this ^{7}Li peak was observed at 11.48 MHz and was left out from Fig. 1. The spectra of the three samples were recorded as a function of τ. The intensity of the $\nu_\alpha(^{11}\text{B})+\nu_\beta(^{11}\text{B})$ peak in the $B_2O_3Li_2O$ glass varied with τ, but a split of this peak was never obtained as in case of the a- and c-B_2O_3 (Fig. 1).

The utilization of the 4P 1D ESEEM spectroscopy can be accomplished through the extraction of the parameters from the spectrum describing the $BOHC_2$ structure. The simulation of the spectrum requires a computer program, not trivial, on the basis of the general expression:[22,23]

$$E(\tau,t_1,t_2)=\frac{1}{8I+4}\sum_{ij,kl}\{C^\alpha_{ik,\ln}(\tau)e^{-i\omega^\alpha_{ik}t_2}e^{-i\omega^\beta_{\ln}t_1}$$
$$+C^\beta_{ik,\ln}(\tau)e^{-i\omega^\alpha_{ik}t_1}e^{-i\omega^\beta_{\ln}t_2}\},$$

where

$$C^\alpha_{ik,\ln}(\tau)=\sum_{jm}M_{il}M^*_lM_{jn}M^*_{kn}M_{km}M^*_{jm}$$
$$\times\{e^{-i(\omega^\alpha_{ij}+\omega^\beta_{lm})}+e^{-i(\omega^\alpha_{kj}+\omega^\beta_{nm})}\}$$

and

$$C^\beta_{ik,\ln}(\tau)=\sum_{jm}M_{il}M^*_lM_{jn}M^*_{kn}M_{km}M^*_{jm}$$
$$\times\{e^{-i(\omega^\alpha_{ij}+\omega^\beta_{lm})}+e^{-i(\omega^\alpha_{kj}+\omega^\beta_{nm})}\}.$$

In the above expression, M_{ij} is the EPR transition amplitude from i sublevel within the α electron spin manifold to the j sublevel within the β manifold. $\omega_{ij}=\omega_i+\omega_j$ is the frequency of nuclear transition between the i and j nuclear sublevels within the same electron spin manifold.[22,23] A FORTRAN program was written for the calculation of the 4P 1D ESEEM spectra based on the above formalism. The program includes also the Euler angles ($\angle a$, $\angle b$, $\angle c$) and ($\angle u$, $\angle v$, $\angle w$) between g and A tensors and g and Q tensors, respectively. This simulation procedure was extensively described in Ref. 7. In this paper,[7] it has been reported that $\angle v(g-Q)=70°$. In the 4P 1D ESEEM spectrum, the selection of angle [$\angle v(g-Q)=70°$] was also the prerequisite to achieve a fitting of the experimental data. Several efforts were completed to find the correct parameters for the reproduction of the experimental spectrum. Figure 1 includes the three theoretical 4P 1D ESEEM spectra resulted from the input data included in the figure.

B. HYSCORE spectroscopy

Figure 2 shows the HYSCORE spectra of the glass recorded with $\tau=168$(A) and 240 (B) nsec. A broad peak [<1.7 MHz (A) and <1.3 MHz (B)] was recorded in the positive quadrant (+,+) around the Larmor frequency of ^{11}B. In addition to the ^{11}B peak, cross peaks were obtained attributed to ^{7}Li and to ^{10}B. These two nuclei will not be

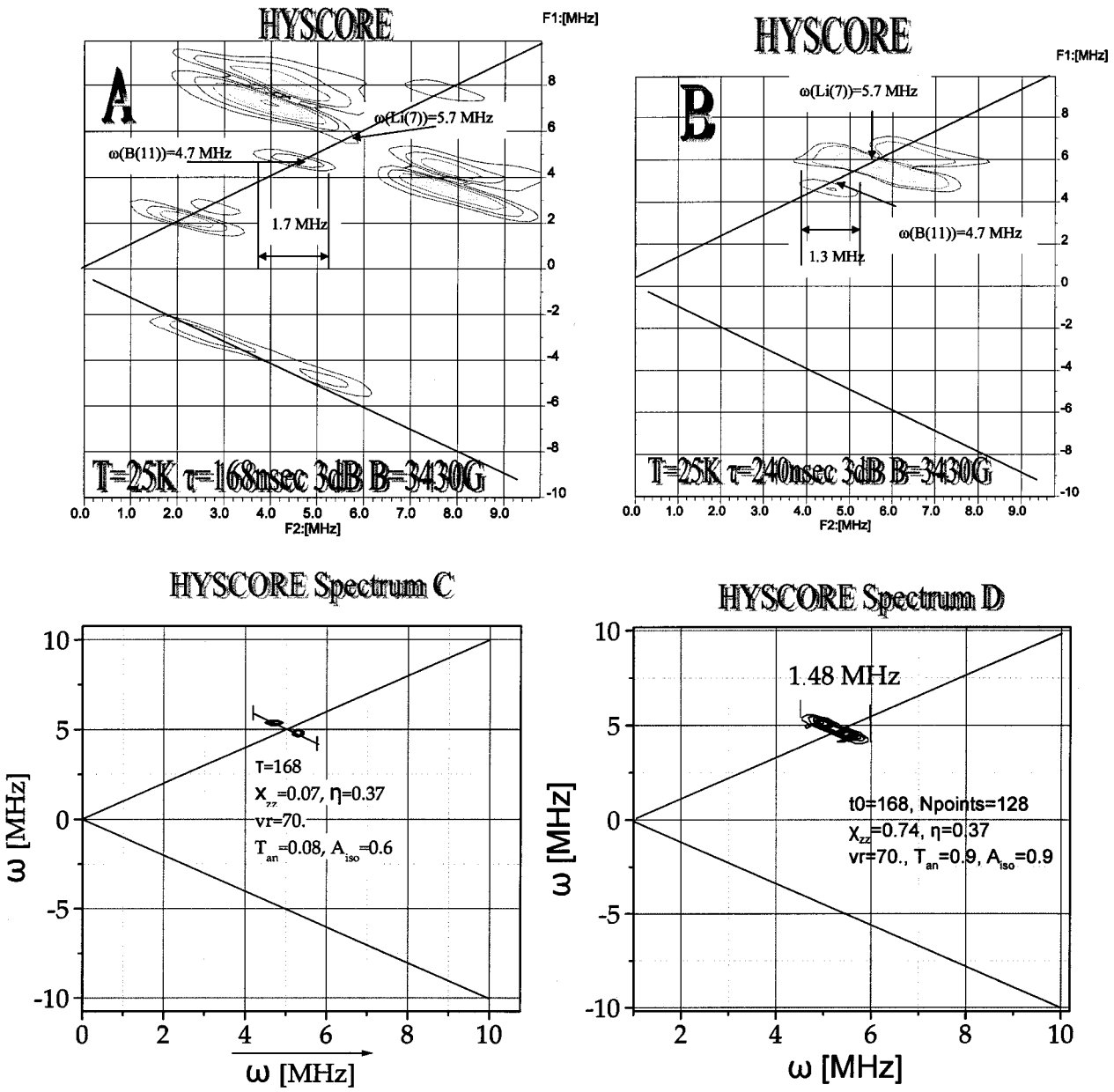

FIG. 2. HYSCORE spectra of the borate glasses with $x=50$ recorded at low temperature and $\tau=168$ (a) and 240 (b) nsec together with three simulated spectra (c) and (d). Input data for HYSCORE calculations: $\tau=168$ nsec, N points$=128$, $\omega_I=4.7820$ MHz, $g_x=2.0049$, $g_y=2.0092$, $g_z=2.0250$, $\angle v\ (g-Q)=70°$, and $\eta=0{,}37$.

discussed more for obvious reasons. Figures 2(c) and 2(d) show the theoretical spectra of ^{11}B calculated using the following input data of included in the figures and procedure described in previous papers.[7-14]

The HYSCORE spectrum obtained using the parameters $\chi_{zz}=0.07$ MHz, $A_{\rm iso}=0.6$ MHz, and $T=0.08$ MHz exhibits two well-resolved peaks due to single quantum transitions (e.g., $\frac{1}{2}\leftrightarrow-\frac{1}{2}$). The variation of $A_{\rm iso}$ between 0 and 1.7 MHz (keeping the other parameters constant) can generate the broad cross peak at $\omega_I=4.78$ MHz of Figs. 2(a) and 2(b). This can be accomplished assuming a range of couplings $\langle A_{\rm iso}\rangle$ for the second boron neighbor of the paramagnetic state due to a loose connection to the site trapping the spin.

The last theoretical calculation [Fig. 2(d)] was done using $\chi_{zz}=0.74$ MHz, $A_{\rm iso}=0.9$ MHz, and $T=0.9$ MHz. Here, the input values correspond to the range of parameters expected from the simulation of the 4P ESEEM spectroscopy. The cross peak now broaden centered along the $\omega_I=4.78$ MHz frequency (perpendicular to the diagonal). The theoretical HYSCORE peak at ω_I obtains a width comparable to the width of the experimental cross peak around the $\omega_I=4.78$ MHz frequency [Figs. 2(a) and 2(b)]. This peak was generated by single quantum transitions (e.g., $-\frac{1}{2}\leftrightarrow\frac{1}{2}$) Again, a better fit can be obtained assuming distribution of $A_{\rm iso}$ and $T_{\rm aniso}$.

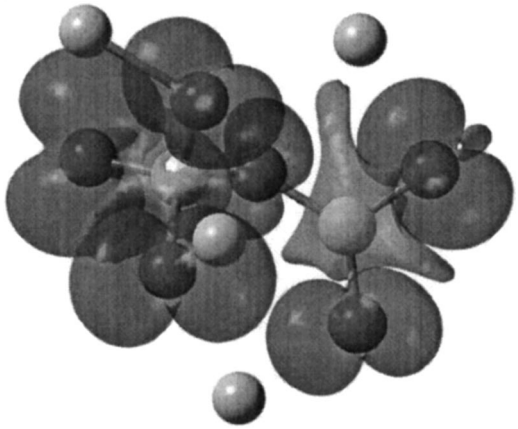

FIG. 3. A combination of a BO_3 and a BO_4 unit acting as a trap center.

This theoretical work signifies that 4P 1D ESEEM and HYSCORE spectroscopies can be used as balancing techniques to pull out the parameters of a paramagnetic state with greater confidence. This combination is important for the evaluation of the structure of defects in the amorphous state because their structure is by nature complicated obstructing advancement in the field of EPR spectroscopy.

C. Quantum mechanical calculations for A_{iso}, χ_{zz}, and η

The interpretation of the spectroscopic data inferred from the CW-EPR, 4P 1D ESEEM, and HYSCORE measurements require the use of quantum mechanical methods yielding the A_{iso}, χ_{zz}, and η parameters for various structures. In previous studies,[7-14] the B3LYP method was used for the calculation of A_{iso} in a number of boron related structures. This method was tested in a- and c-B_2O_3 using results for A_{iso} determined by CW-EPR, 4P ESEEM, HYSCORE, and pulse-ENDOR measurements. In the present study, we tested out the B3LYP method comprehensively for the calculation of the nuclear quadrupole coupling constants (NQC) χ_{zz}, in MHz, and asymmetry parameter (η). In order to reduce the length of the paper, assess the trustworthiness of the method and at the same time to make the article readable, the results of the calculations were appended to this paper (Appendixes A, B, C, and D). Again, the B3LYP method utilized the G98W program that provides the electric field gradient (EFG) q_{xx}, q_{yy}, and q_{zz} in atomic units through calculation of the ground state wave function ψ_0:

$$q_{zz}=\langle \phi_0 | \frac{3z^2-r^2}{r^5} | \phi_0 \rangle .$$

TABLE II. A_{iso}, χ_{zz}, and η parameters for a $H_2O_2BOBO_3H_3$ unit trapping the unpaired electron.

^{11}B	η	χ_{zz} [MHz]	A_{iso} [MHz]
1	0.90	0.22	−12.98
6	0.70	2.20	−16.65

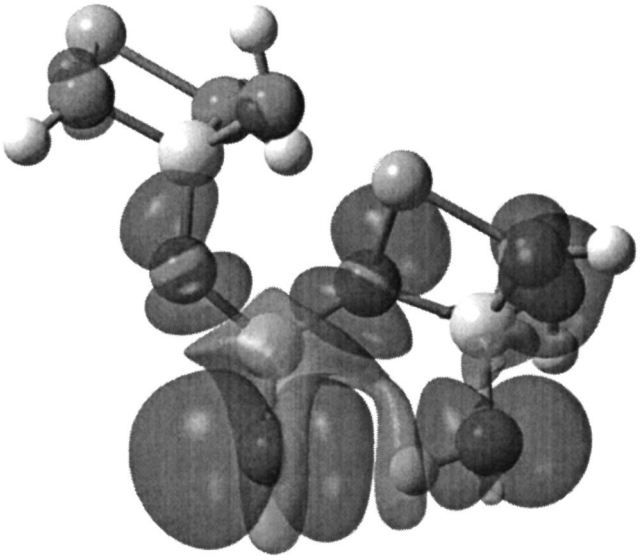

FIG. 4. A BO_3 unit and two BO_4 units generating a site trapping the spin.

The q_{zz} parameter trails a z^2/r^5 dependence causing its rapid fall with the distance. Therefore, the effect of long distant ions on q_{zz} would be small, as it will be shown in the following. The EFG can be converted into the χ_{zz} using the isotropic quadrupole moment Q_I (in b [10^{-28} m^2]) and the equation

$$\chi_{zz}=\frac{e^2 Q_I q_{zz}}{h}=234{,}96\times Q_I \times q_{zz},$$

$$\eta=\left|\frac{q_{xx}-q_{yy}}{q_{zz}}\right|$$

In recent years, several papers published results on χ_{zz} and η in a number of molecules including boron compounds.[30–34] The agreement between theoretical and experimental values for χ_{zz} and η depends on the size of the molecular orbital basis set and the level of refinement of calculation.[30–39]

The evaluation was accomplished through the EFG conversion into χ_{zz} and η values and the comparison of these parameters with experimental values of several compounds.[32] The Q_I value was taken to be 0.040 b from the EPR-ENDOR frequency table of Bruker.[40] In Appendix A, the results of theoretical calculations have been compared

TABLE III. A_{iso}, χ_{zz}, and η parameters for an $\bullet OB^1{}^{OB^5O_3H_3Li}_{OB^6O_3H_3Li}$ unit trapping the unpaired electron.

^{11}B	η	χ_{zz} [MHz]	A_{iso} [MHz]
2	0.10	2.42	−37.77
5	0.47	0.30	−4.34
6	0.21	0.22	3.03

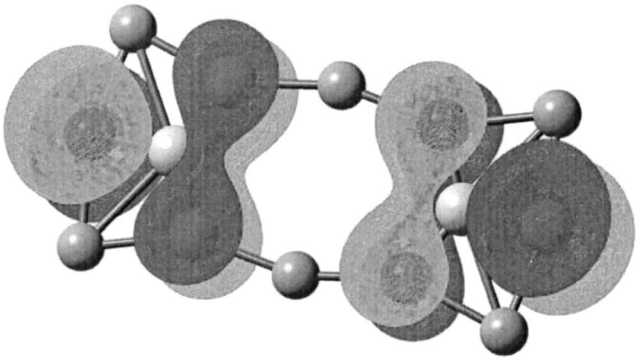

FIG. 5. Couple orthoborate group before irradiations.

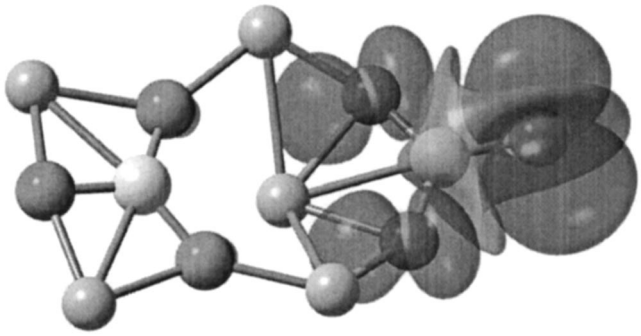

FIG. 6. Couple orthoborate groups after irradiations.

with the experimental values of well-known molecules. Appendixes B and C summarizes the EFG and NQC parameters of simple boron structures both theoretical and experimental derived (NMR and NQR work). In conclusion, the B3LYP method together with the EPR III (for small units) and EPR II (for large units) reproduces the experimental results very well. Until now, the calculations were done in neutral units. The question is how the irradiation alters the EFG and NQC values due to the formation of unpaired states. Appendix D gives the EFG and NQC values of units obtained after irradiation. The changes of the EFG and NQC values are insignificant after irradiation of small units. This implies that experimental parameters deduced from NMR and NQR studies can be directly used for the EPR investigations. Reversibly, the results given in these appendixes are important for the NMR and NQR experimentalists to support their findings. It is worth mentioning here that there are few theoretical studies dealing with the calculation of these parameters.

In the following, calculations serving the scope of the paper are discussed. For example Fig. 3 shows a combination of a boron triangle with a boron tetrahedron resembling the original model for the $BOHC_1$. Table II gives the A_{iso}, χ_{zz}, and η parameters of the original model for the $BOHC_1$.

Furthermore, a single threefold coordinated unit can be bonded to two fourfold coordinated units (Fig. 4).[16] Table III summarizes the A_{iso}, χ_{zz}, and η parameters derived from the optimization process.

In a $1Li_2O\ 1B_2O_3$ glass, two orthoborate groups can be in close proximity. This configuration was named here as couple-orthoborate group. Two orthoborate units were inserted into the G98W program and the resulting structure was optimized by the B3LYP method with the EPR-III basis set. Figures 5 and 6 show the resulting structure before and after irradiation, respectively. Here, the alkali metal helps to form bridges between two nonbridging oxygen atoms. After irradiation, a hole is trapped by nonbridging oxygen

$$\overset{\mathrm{LiO}}{\mathrm{LiO}}\mathrm{B}^{2}\mathrm{O}^{\mathrm{Li}-}_{-\mathrm{Li}}\mathrm{OB}^{8}\overset{\mathrm{OLi}}{\mathrm{OLi}} \overset{\text{irradiation}}{\Rightarrow} \overset{h^{+}\mathrm{O}}{\mathrm{LiO}}\mathrm{B}^{2}\mathrm{O}^{\mathrm{Li}-}_{-\mathrm{Li}}\mathrm{OB}^{8}\overset{\mathrm{OLi}}{\mathrm{OLi}}+[\mathrm{Li}^{+}+e^{-}].$$

The lithium ion can possibly receive the electron, thus becoming neutral. This way, it can move away from the site. This alteration of charge and total number of alkali metal ions of the structure of Fig. 5 causes the remaining ions in the unit to obtain a new equilibrium shown in Fig. 6. A completely different structure occurs in which three alkali metal ions move closer to the center of this compound. Table IV recapitulates the results of this configuration before and after deduction of one alkali metal ion. One can survey slight change of the spectroscopic parameters as a result of irradiation. This change of χ_{ZZ} after irradiation ($\sim 5\%$) can be attributed to the alteration of the effective boron environment and of the change electronic structure as a result of the irradiation.

The orthoborate group can be in the proximity of fourfold coordinated boron loosely attached to this unit. The fourfold coordinated cluster can be part of the network. Figures 7 and 8 show this unit before and after irradiation, respectively. Again, one can perceive from these figures a realignment of the structure after the irradiation. Table V gives the A_{iso}, χ_{zz}, and η parameters before and after irradiation. A 36 and 33 % alteration of the χ_{ZZ} parameter was observed after irradiation of the trigonal and tetragonal boron, respectively. This might be due to the folding of the B^1O_3 triangle towards the B^5O_4 unit. The B^1-B^5-equilibrium distance was calculated to be ~ 4 Å (Fig. 8). Assuming that the center of gravity of the unpaired state is placed on the B^1 site, one would expect $T_{aniso} \sim 0.4$ MHz based on the point dipole approximation ($T = g\mu_\beta g_1 \mu_1 / hr^3$).

In order to complete the discussion, a boroxol group was optimized and the spectroscopic parameters were calculated by the same procedure as above. Figure 9 shows the structure of the $BOHC_{1\alpha}$ defect resulted by this optimization. Table VI gives the A_{iso}, χ_{zz}, and η parameters of this boroxol structure with two boron triangles attached to the ring.

In addition, a boroxol group with three BO_2H_2 triangles was also optimized (6–311 G) and the χ_{zz} parameters were calculated (EPR-III). The χ_{ZZ} [MHz] parameters obtained average values of 2.79 and 2.33 MHz inside and outside the boroxol ring, respectively. This result confirms recent NQR

TABLE IV. A_{iso}, χ_{zz}, and η parameters for two orthoborate units in the proximity.

Before irradiation			After irradiation		
^{11}B	η	χ_{zz} [MHz]	η	χ_{zz} [MHz]	A_{iso} [MHz]
2	0.07	2.83	0.20	−2.65	−30.31
8	0.07	2.83	0.05	−2.72	−0.1

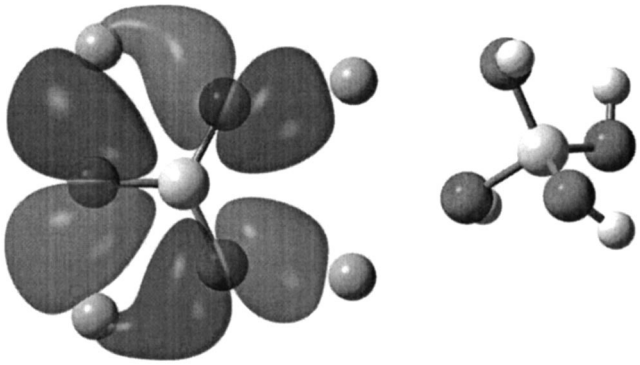

FIG. 7. Orthoborate group close to fourfold coordinated boron before irradiations.

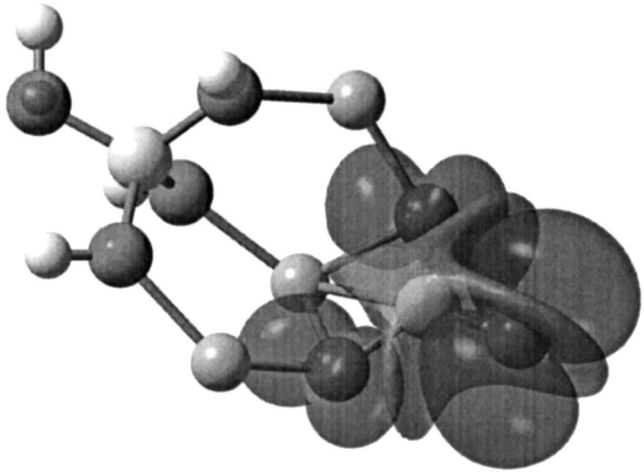

FIG. 8. Orthoborate groups close to fourfold coordinated boron after irradiations. The optimization was accomplished by using the B3LYP method and the 6-311+G basis set instead of the EPR-III basis set due to long computation time.

work on borate glasses by Bray.[41] Bray observed two NQR frequencies in vitreous B_2O_3 at 1358 and 1308 kHz due to two dissimilar sites, namely boron inside and outside the boroxol ring (3.5% effect), respectively.[41–44] The quadrupole parameters of boron within the boroxol ring have not been affected by the irradiation significantly as in the case of the structure composed of the couple-orthoborate group. The χ_{zz} and η parameters of the boroxol ring are the same as the isolated $BO_3(H_3,Li_3)$ unit and also the same as the values reported by the NMR and NQR work of Bray and collaborators in vitreous B_2O_3 (Table VII).

IV. DISCUSSION

There is significant work concerning the evaluation of the different structures in borate glasses occurring as a function of R (molar percentage of the alkali oxide to the molar percentage of boron oxide). In the region of $R\sim1$, threefold coordinated units coexists with fourfold coordinated boron units according to the NMR literature.[44–51] In addition, Raman studies in glasses with high alkali content have shown the coexistence of pyroborate and orthoborate units.[52] These units provide the potential precursors of the $BOHC_2$ defect.

The proposed structure for the $BOHC_2$ defect should consists of units explaining the present and previous EPR experimental work[1–19] based on structures occurring in this region of composition.[41,44,47] The EPR spectroscopic parameters concern (1) the g values of the $BOHC_2$ (Table I),[1–19] (2) the spin lattice relaxation of the $BOHC_2$,[16] (3) the quadrupole parameter of the $BOHC_2$ (Ref. 16, 4P 1D ESEEM and HYSCORE results), (4) the A_{iso} of the first (Table I),[1–19] and second boron neighbor (4P 1D ESEEM and HYSCORE results), and (5) the T_{aniso} of the second neighbor (4P 1D ESEEM and HYSCORE results).

The theoretical study of this work has shown that the A_{iso} of the unpaired state interacting with the first boron neighbor results in couplings greater than $|29|$ MHz and less than $|21|$ MHz when boron is threefold or fourfold coordinated, respectively. This result is in accordance with previous theoretical work.[8–14,18] Since A_{iso} is equal to 30.1 MHz for $BOHC_2$ (Table I), the unpaired electron must be localized at nonbridging oxygen connected to threefold coordinated boron. There are three candidates that can be sorted out from the assortment of the above calculation for the justification of CW-EPR result. The first contestant could be the pyroborate group, the second applicant may well be the coupled orthoborate group and the third contender could be the orthoborate unit close to a fourfold coordinated unit.

HYSCORE spectroscopy furnished a weak A_{iso} for the second neighbor with values between 0 and 0.9 MHz [Figs. 2 (c) and 2(d)]. The theoretical calculations revealed that NQC is less than ~0.74 MHz. On the ground of these observations for A_{iso} and NQC, the pyroborate group ($A_{iso}=5.2$ MHz and $\chi_{zz}=2.67$ MHz) can be excluded. Explicitly, it is expected to produce one set of HYSCORE peak because it exhibits $A_{iso}=5.2$ MHz for the second neighbor. The HYSCORE spectra of the a- and c- B_2O_3 yielded two narrow and well-resolved cross peaks.[7–14] Specifically, two sharp cross peaks were resolved with separation of 6 and 2 MHz for a-B_2O_3.[7] One narrow and well resolved cross peak with separation of 6 MHz was obtained by HYSCORE for the c-B_2O_3.[7–14] These couplings were associated with NQC equal to 2.7 MHz. This strong quadrupole interaction affects

TABLE V. A_{iso}, χ_{zz}, and η parameters for one orthoborate unit in the proximity of a BO_4 unit.

Before irradiation			After irradiation					
^{11}B	η	χ_{zz} [MHz]	η	χ_{zz} [MHz]	A_{iso} [MHz]	T_{xx} [MHz]	T_{yy} [MHz]	T_{zz} [MHz]
1	0.03	2.78	0.70	−1.80	−30.354	−8.27	−2.71	10.98
5	0.15	0.28	0.18	0.35	−0.005	−0.197	−0.196	0.393

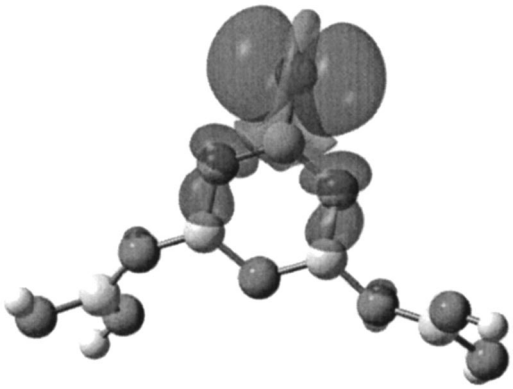

FIG. 9. A boroxol group with two BO_2H_2 units acting as a trap of the spin.

strongly the $\frac{3}{2}$-states that are smeared additionally due to the random distribution of the sites in the glass. Therefore, the HYSCORE spectra originated by strong NQC in borate glasses are due to $\frac{1}{2} \leftrightarrow -\frac{1}{2}$ transitions for $A_{iso} < 2\,\omega_I$. Here, the pyroborate group may well exhibit NQC of ~ 2.67 MHz and one weak coupling with $A_{iso} = 5.20$ MHz. It is expected that the HYSCORE spectra of the pyroborate group would consist of cross peaks around the Larmor frequency of ^{11}B.

The other possibility consists in the couple orthoborate group because the strong coupling was estimated to be $A_{iso} = -30.31$ MHz (Table IV). This unit processes $A_{iso} = -0.1$ MHz and $\chi_{zz} = 2.72$ MHz for the second neighbor (Table IV). The $B^2 - B^8$ distance is 4.3 Å according to the calculation. This would result in a $T_{aniso} \sim 0.35$ MHz based on the point dipole approximation assuming the B^2 atom as center of gravity of the unpaired state. Although A_{iso} and T_{aniso} are within the experimental expected values; the χ_{zz} parameter is far outside the expected value. The experimental value of $\chi_{zz\sim}$ 0.74 MHz suggests fourfold coordinated boron for the second neighbor (Table VIII).

The HYSCORE spectrum of the $1Li_2O\ 1B_2O_3$ sample can be generated by a structure that is flexible to induce smearing of the cross peaks. This flexibility can be obtained by the orthoborate group close to fourfold coordinated boron (Fig. 8). The resulted spectroscopic parameters from the simulation are within the experimental expected values.

The 4P 1D ESEEM spectra of the a- and c-B_2O_3 and $1Li_2O\ 1B_2O_3$ glass are dissimilar. The a- and c-B_2O_3 materials exhibit a splitted double frequency peak (Fig. 1). When an element exhibits a quadrupole moment Q, one expects a splitting of the double frequency 4P 1D ESEEM peak with a separation δ:[22,23]

$$\delta = \frac{3}{2}\frac{e^2qQ}{h}(3\cos^2\theta - 1)$$

which is affected by the size and orientation of the NQC tensor with respect to the complex coordinate system.[22,23] Taking $\delta \sim 0.45$ MHz for c- and a-B_2O_3 and $\theta = 70°$ (Fig. 1),[22,23] χ_{zz} becomes ~ 2.62 MHz for the second neighbor for the $BOHC_{1\alpha,\beta,\gamma}$ (compare Table VI). This value is very

TABLE VI. A_{iso}, χ_{zz}, and η parameters for the boroxol structure with two boron triangles generating the $BOHC_{1\alpha}$ defect.

^{11}B	η	χ_{zz} [MHz]	A_{iso} [MHz]
1	0.16	2.71	6.87
4	0.18	2.66	5.52
5	0.21	2.63	−32.36

rough because the 4P 1D ESEEM spectra were not simulated to observe the accurate values for χ_{zz}. This is time consuming and has been reserved for another publication. Nevertheless, the estimated value from the spectra of Fig. 1 is in excellent agreement with previous work[7–14] expected by the result of the theoretical calculation for $BOHC_{1\alpha}$ of Fig. 9 (compare Table VI). The 4P 1D ESEEM experiments demonstrate that they can become a powerful tool to probe the environment of defects in glasses and provide significant information about the amorphous state.

Since a splitting was not observed in the 4P 1D ESEEM spectrum of the $1Li_2O\ 1B_2O_3$ glass, the δ splitting would be less than 0.2 MHz implying that the value for χ_{zz} is less than 1.1 MHz. The simulation of the 4P 1D ESEEM spectrum gives for χ_{zz} the value of less than 0.74 MHz, which is in the range of the expectation.

NMR and NQR spectroscopies give the following two ranges for NQC in crystalline borates[41,44] (Table VIII).

These results guide to the conclusion that the second neighbor of boron would be fourfold coordinated. This situation pinpoints the structures of Figs. 4 and 8 because they can explain the NQC. The structure of Fig. 4 predicts $A_{iso} \sim -38$ MHz, $A_{iso} = -4.34$ MHz, and $A_{iso} = 3.03$ MHz (Table III) exceeding the value of $A_{iso} = 30.1$ MHz and $A_{iso} \sim 0.9$ MHz [Table I and Fig. 2(d)] obtained by the simulation of the CW-EPR spectrum and HYSCORE spectra, respectively.

The A_{iso}, χ_{zz}, and η parameters derived from the simulation of the 4P 1D ESEEM program are close to the structure consisting of one orthoborate group close to a fourfold coordinated boron (Table V and Fig. 8). Allowing a variation of χ_{zz} and A_{iso} due to the flexibility provided by the structure of Fig. 8, one could expect a far better fit of the 4P 1D ESEEM spectrum. Nevertheless, the agreement between theory and experiment is satisfactory for the needs of this discussion. The results of the HYSCORE and 4P 1D ESEEM experiments can tentatively be explained by the structure of Fig. 8.

This structure can also explain the shift of the $g_1 = 2.0049$ from the $g_e = 2.0023$. The $BOHC_1$ possesses $g_1 = 2.002$ close to the free electron (Table 1). The models pro-

TABLE VII. ^{11}B quadrupole parameter in a-B_2O_3 (Refs. 37, 44).

	NMR 300 K	NQR 300 K	NQR 77 K
Q_{cc}	2690 ± 30 kHz	2682.6 ± 0.5 kHz	2701.1 ± 0.2 kHz
η	0.06 ± 30	0.071 ± 0.001	0.076 ± 0.001

TABLE VIII. Ranges of values in the amorphous materials for threefold and fourfold coordinated boron (Refs. 41, 44).

B coordination	χ_{zz} [MHz]	Comments	η
Tetragonal	0–0.855	N_4	0–1
		Symmetric group either 3 bridging or else 3 nonbridging oxygens with OH treated as bridging oxygen, N_3S	0–0.23
Trigonal	2.45–2.81	N_3	
		Asymmetric group containing 1 N_3A_1 or 2 N_3A_2 nonbridging oxygens	0.47–0.75

posed for the $BOHC_{1\alpha,\beta,\gamma}$ (Refs. 7–14) (Fig. 9) allow nearly all spin density of the unpaired state to be localized at the nonbridging oxygen.[7] In silicate glasses, the HC_1 can be described by an unpaired electron localized completely at the nonbridging oxygen.[5] In this case, g_1 is equal to 2.003.[5] Here, the model of Fig. 8 indicates significant delocalization of the unpaired state to the other two nonbridging oxygen ions. As in case of the $BO_3{}^{2-}\bullet$ defect in potassium borate ceramics where a $g_1=2.009$ was reported,[6] the shift of the g_1 value from g_e value was attributed to the delocalization of the spin density over the other oxygen ions. Due to the similarity of the species, the same mechanism should be present here accounting for the shift g_1 of $BOHC_2$ away from g_e. As in case of the $BOHC_{1\alpha,\beta,\gamma}$ center, there might also be $BOHC_{2n}$ variants. The present measurements cannot provide such evidence. High frequency measurements would be needed to eventually separate these components, if present.

Shkrob *et al.*[16] determined that the spin lattice relaxation of the $BOHC_1$ and $BOHC_2$ are very similar. Kordas[53] measured the spin lattice relaxation time T_1 of variants of the E_1' center in silica fiber tubes. In this material, three centers were observed the one of which was attributed to the E_1' center. The other two exhibit an hyperfine splitting of 75 and 420 G due to the interaction of the E_1' center with a hydrogen (H-E_1' center) and the nucleus of ^{29}Si (^{29}Si-E_1' center), respectively. T_1 was measured between 10 and 300 K. The temperature variation of T_1 was the same for the three defects in the region between 40 and 300 K. The variation of T_1 with temperature was explained by assuming thermal vibrations of the lattice. The square well box model described them. The identity of T_1 with T was explained by the similarity of the structure of the three defects. Only defects with similar structures can produce square well potentials that would establish energies and resonance frequencies generating nearly identical T_1.[53–56] Based on that finding, the 420 G doublet was attributed to the interaction of the E_1' center with the nucleus of ^{29}Si.[53] The E_1' center was described by an electron trapped by a silicon which faces the oxygen vacancy.[53] It is expected that the same mechanism would determine T_1 in borate glasses. According to the box model,[53–56] the short-range order determines T_1. In the case of the $1Li_2O\ 1B_2O_3$ glass; the orthoborate group would affect most significantly T_1 as the boron triangle in the $BOHC_{1\alpha,\beta,\gamma}$ defect. This measurement provides additional evidence that the local structure of this defect would be a BO_3 unit.

V. CONCLUSION

The 4P 1D ESEEM and HYSCORE spectroscopies resulted in the determination of the χ_{zz} and A_{iso} parameters of the second neighbor. The theoretical work gave a number of different structures, though the one consisting of an orthoborate unit close to a fourfold coordinated unit reproduces the experimental work more reasonable. This structure allows delocalization of the unpaired state over the three nonbridging oxygen but not equally. This delocalization produces the shift of g_1 from g_e. All these experimental facts including the spin-lattice relaxation time T_1 and the g_1 shift can be explained by the structure composed of an unpaired electron trapped by an orthoborate group attached to another fourfold coordinated unit. Here, two different pulsed EPR methods were employed to extract the spectroscopic parameters of the unpaired state. This equivalent use of the methods gives more comfort to the experimentalist to extract the spectroscopic parameters of the FT-EPR spectra obtained in glasses that are complicated by their nature alone. Most of all, the 4P ESEEM was employed in glasses the first time in literature.

ACKNOWLEDGMENTS

The author thanks Dr. G. Jeschke at the Max Planck Institute for Polymer Research (Mainz, Germany) for his advice concerning the computation of the EFG tensor and the references relating to the published 4P 1D ESEEM work that is in short supply. In addition, I show appreciation to A. Kokinos for preparing the samples. I am also grateful to the General Secretariat for Research and Technology in Greece for generous funding of the FT-EPR Bruker instrument and of my research on glass science and technology (several STRIDE and EIIET II programs) for the last ten years in Greece.

APPENDIX A

Calculated and experimental values of χ_{zz} and η for BF_2OH_2, BF_3, BH_2OH, and BH_3-NH_3.

		Electric field gradient for BF_2-OH_1					
^{11}B	Method	q_{xx} [a.u.]	q_{yy} [a.u.]	q_{zz} [a.u.]	η	χ_{zz} [MHz]	Reference
	SCF-TZVP	0.102	0.213	−0.315	0.35	−2.964	32
1	MW					2.672	32
1	B3LYP-6-311G	0.163	0.053	−0.216	0.51	−2.031	Present
1	B3LYP-6-311+G	0.166	0.049	−0.215	0.54	−2.024	Present
1	B3LYP-6-311++G	0.163	0.053	−0.216	0.51	−2.031	Present
1	B3LYP-EPR-III	0.195	0.082	−0.277	0.41	−2.599	Present
		Electric field gradient for BF_3					
^{11}B	Method	q_{xx} [a.u.]	q_{yy} [a.u.]	q_{zz} [a.u.]	η	χ_{zz} [MHz]	Reference
	SCF-TZVP	0.1634	0.163	−0.327	0	−3.071	32
1	NQR					2.690	32
1	B3LYP-6-311G	0.117	0.117	−0.234	0	−2.202	Present
1	B3LYP-6-311+G	0.166	0.049	−0.215	0.54	−2.024	Present
1	B3LYP-6-311++G	0.116	0.116	−0.232	0	−2.185	Present
1	B3LYP-EPR-III	0.148	0.148	−0.297	0	−2.791	Present
		Electric field gradient for BH_2OH					
^{11}B	Method	q_{xx} [a.u.]	q_{yy} [a.u.]	q_{zz} [a.u.]	η	χ_{zz} [MHz]	Reference
	SCF-TZVP	0.174	0.307	−0.481	0.28	−4.520	32
1	MW					3.900	32
1	B3LYP-6-311G	0.315	0.130	−0.445	0.42	−4.184	Present
1	B3LYP-6-311+G	0.325	0.127	−0.452	0.44	−4.246	Present
1	B3LYP-6-311++G	0.325	0.127	−0.452	0.44	−4.247	Present
1	B3LYP-EPR-III	0.327	0.166	−0.493	0.33	−4.633	Present
		Electric field gradient for BH_3-NH_3					
^{11}B	Method	q_{xx} [a.u.]	q_{yy} [a.u.]	q_{zz} [a.u.]	η	χ_{zz} [MHz]	Reference
	SCF-TZVP	0.150	0.150	−0.300	0	−2.815	32
1	B3LYP-6-311G	0.153	0.153	−0.306	0	−2.874	Present
1	B3LYP-6-311+G	0.154	0.153	−0.307	0	−2.885	Present
1	B3LYP-6-311++G	0.154	0.153	−0.307	0	−2.885	Present
1	B3LYP-EPR-III	0.166	0.166	−0.332	0	−3.117	Present
		Electric field gradient for HBF_2					
^{11}B	Method	q_{xx} [a.u.]	q_{yy} [a.u.]	q_{zz} [a.u.]	η	χ_{zz} [MHz]	Reference
	SCF-TZVP	0.096	0.314	−0.410	0.53	−3.847	32
1	NQR					3.148	32
1	B3LYP-6-311G	0.043	0.305	−0.348	0.80	−3.273	Present
1	B3LYP-6-311+G	0.041	0.311	−0.352	0.77	−3.308	Present
1	B3LYP-6-311++G	0.041	0.311	−0.352	0.77	−3.308	Present
1	B3LYP-EPR-III	0.084	0.315	−0.399	0.58	−3.746	Present

SCF were performed with GAMES and the CI by DIRECT. TZVP=triple-zeta valence+polarization according to the Dunning recipes.

APPENDIX B

EFG and NQC parameters for the BO_3H_3 and BO_3Li_3 structures.

^{11}B in BO_3H_3	Method	q_{xx} [a.u.]	q_{yy} [a.u.]	q_{zz} [a.u.]	η	χ_{zz} [MHz]
1	AM1	0.119	0.119	−0.238	0	−2.239
1	B3LYP-6-311G	0.110	0.110	−0.220	0	−2.069
1	B3LYP-6-311+G	0.111	0.111	−0.222	0	−2.091
1	B3LYP-6-311++G	0.111	0.111	−0.222	0	−2.090
1	B3LYP-EPR-II	0.129	0.129	−0.259	0	−2.434
1	B3LYP-EPR-III	0.142	0.142	−0.284	0	−2.669
1	MRPW1PW91-6-311G	0.111	0.111	−0.223	0	−2.096
^{11}B in BO_3Li_3	Method	q_{xx} [a.u.]	q_{yy} [a.u.]	q_{zz} [a.u.]	η	χ_{zz} [MHz]
1	AM1	0.159	0.159	−0.318	0	−2.985
1	B3LYP-6-311G	0.113	0.113	−0.226	0	−2.120
1	B3LYP-6-311+G	0.113	0.113	−0.225	0	−2.119
1	B3LYP-6-311++G	0.113	0.113	−0.225	0	−2.119
1	B3LYP-EPR-III	0.159	0.159	−0.318	0	−2.757

APPENDIX C

NQC and asymmetry parameters for the pyroborate group ($H_2O_2B^1OB^5O_2H_2$) optimized by the B3LYP-EPR-III method and work from Tossel (Refs. 30, 31).

^{11}B	η	χ_{zz} [MHz]	Literature
1	0.03	2.71	Present
5	0.47	2.55	Present
1		2.35	3-21G (Ref. 30)
5		2.33	3-21G (Ref. 30)
1		2.98	6-311G(2d) (Ref. 30)
5		3.03	6-311G(2d) (Ref. 30)

NQC and asymmetry parameters for the metaborate group using the B3LYP-EPR-III method in comparison with the experimental NQC parameters reported for the metaborate group.[48]

^{11}B	η	χ_{zz} [MHz]	Literature
1	0.60	2.53	Present
5	0.52	2.67	Present
8	0.18	2.72	Present
Average	0.43	2.64	Present
	Compound		
$Li_2OB_2O_3$	0.55	2.58	48
$CaOB_2O_3$	0.55	2.58	48
$Na_2OB_2O_3$	0.75	2.45	48
$SrOB_2O_3$	0.51	2.57	48
Average	0.59	2.55	48

APPENDIX D

A_{iso}, χ_{zz}, and η parameters for an orthoborate structure trapping the unpaired electron.

^{11}B	η	χ_{zz} [MHz]	A_{iso} [MHz]
1	0.20	2.44	−37.37

A_{iso}, χ_{zz}, and η parameters for a pyroborate structure trapping the unpaired electron.

^{11}B	η	χ_{zz} [MHz]	A_{iso} [MHz]
1	0.20	2.67	5.20
5	0.64	2.56	−30.03
Average	0.42	2.62	

A_{iso}, χ_{zz}, and η parameters for a metaborate structure with three BO_3 units trapping the unpaired electron.

^{11}B	H	χ_{zz} [MHz]	A_{iso} [MHz]
1	0.40	2.61	−38.49
5	0.41	2.67	5.92
8	0.28	2.70	−0.038
Average	0.36	2.66	

A_{iso}, χ_{zz}, and η parameters for a BO_4H_4 unit trapping the unpaired electron.

^{11}B	η	χ_{zz} [MHz]	A_{iso} [MHz]
1	1.00	0.13	−21.49

*Electronic address: gkordas@ims.demokritos.gr

[1] D.L. Griscom, P.C. Taylor, D.A. Ware, and P.J. Bray, J. Chem. Phys. **48**, 5158 (1968).
[2] D.L. Griscom, G.H. Sigel, Jr., and R.J. Ginther, J. Appl. Phys. **47**, 960 (1976).
[3] P.C. Taylor and D.L. Griscom, J. Chem. Phys. **55**, 3610 (1971).
[4] M.C.R. Symons, J. Chem. Phys. **53**, 468 (1970).
[5] D.L. Griscom, P.C. Taylor, and P.J. Bray, J. Chem. Phys. **53**, 469 (1970).
[6] P.C. Taylor, D.L. Griscom, and P.J. Bray, J. Chem. Phys. **54**, 748 (1971).
[7] Y. Deligiannakis, L. Astrakas, and G. Kordas, Phys. Rev. B **58**, 11420 (1998).
[8] G. Kordas, Phys. Chem. Glasses **41**, 325 (2000).
[9] G. Kordas in First ENDEASD WORKSHOP, edited by C. Claeys, Santorini, Greece, April 21-22 (1999), 82.
[10] G. Kordas, Phys. Chem. Glasses **41**, 1 (2000).
[11] G. Kordas, Phys. Chem. Glasses **41**, 358 (2000).
[12] G. Kordas, J. Non-Cryst. Solids **260**, 75 (1999).
[13] G. Kordas in Proceedings of the Second International Conference on Borate Glasses, Crystals, and Melts, edited by A.C. Wright, S.A. Feller, and A.C. Hannon, 1997, pp. 148-155.
[14] G. Kordas, Phys. Chem. Glasses **39**, 21 (1996).
[15] I.A. Shkrob and V.F. Tarasov, J. Chem. Phys. **113**, 10723 (2000).
[16] I.A. Shkrob, B.M. Tadjikov, and A.D. Trifunac, J. Non-Cryst. Solids **262**, 6 (2000).
[17] B. Boizot, G. Petite, D. Ghaleb, and G. Galas, J. Non-Cryst. Solids **283**, 179 (2001).
[18] G. Kordas, Phys. Chem. Glasses **42**, 226 (2001).
[19] D.L. Griscom, in *Experimental Techniques of Glass Science*, edited by C.J. Simmons and El-Bayoumi (American Ceramic Society, Westerville, OH, 1993), p. 161, Chap. 6.
[20] C. Gemperle, Ph.D. thesis, ETH Zuerich, 1992, p. 71.
[21] A. Schweiger, in *Modern Pulsed and Continuous Wave ESR*, edited by L. Kevan and M.K. Bowman (Wiley, New York, 1990), p. 52.
[22] A.M. Tyryshkin, S.A. Dikanov, R.G. Evelo, and A.J. Hoff, J. Chem. Phys. **97, 1**, 42 (1992).
[23] A.M. Tyryshkin, S.A. Dikanov, and D. Goldfarb, J. Magn. Reson., Ser. A **105**, 271 (1993).
[24] P. Hoefer, A. Grupp, G. Nebenfuer, and M. Mehring, Chem. Phys. Lett. **132**, 279 (1986).
[25] J.J. Shane, P. Hoefer, E.J. Reijerse, and E. de Boer, J. Magn. Reson. **99**, 596 (1992).
[26] A. Schweiger and G. Jeschke, *Principles of Pulse EPR* (Oxford University Press, New York, 2001), pp. 284–295.
[27] M. J. Frisch, G. W. Trucks, H. B. Schlegel, G. E. Scuseria, M. A. Robb, J. R. Cheeseman, V. G. Zakrzewski, J. A. Montgomery, Jr., R. E. Stratmann, J. C. Burant, S. Dapprich, J. M. Millam, A. D. Daniels, K. N. Kudin, M. C. Strain, O. Farkas, J. Tomasi, V. Barone, M. Cossi, R. Cammi, B. Mennucci, C. Pomelli, C. Adamo, S. Clifford, J. Ochterski, G. A. Petersson, P. Y. Ayala, Q. Cui, K. Morokuma, D. K. Malick, A. D. Rabuck, K. Raghavachari, J. B. Foresman, J. Cioslowski, J. V. Ortiz, A. G. Baboul, B. B. Stefanov, G. Liu, A. Liashenko, P. Piskorz, I. Komaromi, R. Gomperts, R. L. Martin, D. J. Fox, T. Keith, M. A. Al-Laham, C. Y. Peng, A. Nanayakkara, M. Challacombe, P. M. W. Gill, B. Johnson, W. Chen, M. W. Wong, J. L. Andres, C. Gonzalez, M. Head-Gordon, E. S. Replogle, and J. A. Pople, GAUSSIAN 98, Revision A.9 (Gaussian, Inc., Pittsburgh, PA, 1998).
[28] J.B. Foresman and A. Frisch, in *Exploring Chemistry with Electronic Structure Methods*, 2nd ed. (Gaussian, Inc., Pittsburgh, PA, 1993).
[29] V. Barone, in *Recent Advances in DFT Methods*, edited by D.P. Chong (World Scientific, Singapore, 1996), Pt. I.
[30] J.A. Tossel, J. Non-Cryst. Solids **183**, 307 (1995).
[31] J.A. Tossel, J. Non-Cryst. Solids **215**, 236 (1997).
[32] M.H. Palmer, Z. Naturforsch. A **45**, 357 (1990).
[33] M.H. Palmer and J.A. Blair-Frish, Z. Naturforsch. A **49**, 137 (1994).
[34] M. Torrent, D.G. Musaev, K. Morokuma, S-C. Ke, and K. Warncke, J. Chem Soc. B **103**, 8618 (1999).
[35] T-K. Ha, Z. Naturforsch. A **41**, 163 (1986).
[36] N. Bessis, H. Lefebvre-Brion, and C.M. Moser, Rev. Mod. Phys. **35**, 548 (1963).
[37] M.H. Palmer, Z. Naturforsch. A **41**, 147 (1986).
[38] M.H. Palmer, Z. Naturforsch. A **47**, 203 (1992).
[39] J. Murgisch, Y. Aray, and E.O. Tico, Z. Naturforsch. A **47**, 217 (1992).
[40] BRUKER Almanac 2002, p. 36.
[41] P.J. Bray, Inorg. Chim. Acta **289**, 158 (1999).
[42] G.E. Jellison, Jnr., S.A. Feller, and P.J. Bray, Phys. Chem. Glasses **19**, 52 (1973).
[43] G.L. Turner, K.A. Smith, R.J. Kirkpatrick, and E. Oldfield, J. Magn. Reson. **67**, 544 (1986).
[44] P.J. Bray, in *Proceedings of the Second International Conference On Borate Glasses, Crystals and Melts*, edited by A.C. Wright, S.A. Feller, and A.C. Hannon (The Society of Glass Technicians, Sheffield, 1997), p. 1.
[45] H.M. Kriz and P.J. Bray, J. Magn. Reson. **4**, 69 (1971).
[46] D. Kline, P.J. Bray, and H.M. Kriz, J. Chem. Phys. **48**, 5277 (1968).
[47] Y.H. Yun and P.J. Bray, J. Non-Cryst. Solids **44**, 227 (1981).
[48] H.M. Kriz and P.J. Bray, J. Magn. Reson. **4**, 76 (1971).
[49] A.H. Silver, J. Chem. Phys. **32**, 959 (1960).
[50] S.A. Feller, W.J. Well, and P.J. Bray, J. Non-Cryst. Solids **51**, 21 (1982).
[51] A.H. Silver and P.J. Bray, J. Chem. Phys. **29**, 984 (1958).
[52] W.L. Konijnedijk, Ph.D. thesis, 1975.
[53] G. Kordas, Phys. Chem. Glasses **33**, 143 (1992).
[54] F.G. Klemens, Phys. Rev. **138**, 1217 (1965).
[55] D.W. Feldman, J.D. Castle, and J. Murpy, Phys. Rev. **138**, 1208 (1965).
[56] L.K. Aminov, I.N. Kurkin, D.A. Lukoyanov, and K.P. Chemov, Phys. Solid State **39**, 1184 (1997).